Atmospheric ion-induced nucleation of sulfuric acid and water

E. R. Lovejoy
Aeronomy Laboratory, NOAA, Boulder, Colorado, USA

J. Curtius
Institut für Physik der Atmosphäre, Universität Mainz, Mainz, Germany

K. D. Froyd[1]
Aeronomy Laboratory, NOAA, Boulder, Colorado, USA

Received 17 December 2003; revised 24 February 2004; accepted 3 March 2004; published 22 April 2004.

[1] Field studies show that gas phase nucleation is an important source of new particles in the Earth's atmosphere. However, the mechanism of new particle formation is not known. The predictions of current atmospheric nucleation models are highly uncertain because the models are based on estimates for the thermodynamics of cluster growth. We have measured the thermodynamics for the growth and evaporation of small cluster ions containing H_2SO_4 and H_2O, and incorporated these data into a kinetic aerosol model to yield quantitative predictions of the rate of ion-induced nucleation for atmospheric conditions. The model predicts that the binary negative ion H_2SO_4/H_2O mechanism is an efficient source of new particles in the middle and upper troposphere. The ion-induced $HSO_4^-/H_2SO_4/H_2O$ mechanism does explain nucleation events observed in the remote middle troposphere, but does not generally predict the nucleation events observed in the boundary layer. *INDEX TERMS:* 0305 Atmospheric Composition and Structure: Aerosols and particles (0345, 4801); 0317 Atmospheric Composition and Structure: Chemical kinetic and photochemical properties; 0335 Atmospheric Composition and Structure: Ion chemistry of the atmosphere (2419, 2427); 0365 Atmospheric Composition and Structure: Troposphere—composition and chemistry; *KEYWORDS:* nucleation, ions, sulfuric acid

Citation: Lovejoy, E. R., J. Curtius, and K. D. Froyd (2004), Atmospheric ion-induced nucleation of sulfuric acid and water, *J. Geophys. Res.*, *109*, D08204, doi:10.1029/2003JD004460.

1. Introduction

[2] Aerosol is ubiquitous in the Earth's lower atmosphere. It affects human health, visibility, atmospheric chemistry, and climate. Aerosol influences climate directly by scattering and absorbing radiation, and indirectly by acting as cloud droplet nuclei and affecting cloud properties. Gas phase nucleation is an important source of particles in the Earth's atmosphere [*Kulmala et al.*, 2004]. New particle formation is correlated with enhanced levels of gas phase sulfuric acid [*Weber et al.*, 1995, 2001a] and low aerosol surface area (the dominant sulfuric acid sink) [*Clarke*, 1992; *de Reus et al.*, 1998; *Hegg et al.*, 1993; *Perry and Hobbs*, 1994; *Hoppel et al.*, 1994; *Clarke*, 1993; *Covert et al.*, 1992; *Keil and Wendisch*, 2001]. Water is also implicated in the formation of new particles because it is abundant and it significantly suppresses the vapor pressure of sulfuric acid. Nucleation in the background troposphere is common in regions of cloud outflow [*Weber et al.*, 2001b; *Clarke et al.*, 1998a; *Hegg et al.*, 1990; *Keil and Wendisch*, 2001]. These regions are favorable for nucleation due to enhanced solar radiation, high relative humidity (RH), and reduced particle surface area. In the middle and lower troposphere, nucleation frequently occurs where classical binary H_2SO_4/H_2O nucleation theory does not predict new particle formation [*Weber et al.*, 2001a; *Clarke et al.*, 1998b; *Weber et al.*, 1997, 1999]. This has led to the suggestions that other species (e.g., NH_3) are involved [*Weber et al.*, 1998; *Kulmala et al.*, 2000; *Coffman and Hegg*, 1995; *Marti et al.*, 1997], or that an ion mechanism is important [*Yu and Turco*, 2001]. Ion-induced nucleation (IIN) may explain a possible connection between the flux of galactic cosmic rays (the main source of ions in the background atmosphere) and global cloudiness [*Carslaw et al.*, 2002; *Harrison and Carslaw*, 2003]. Field measurements of the mobility spectrum of air ions [*Hõrrak et al.*, 1998] show bursts of intermediate ions (1.6–7.4 nm) that may be associated with ion-induced nucleation. *Eichkorn et al.* [2002] have detected large positive ions in the upper troposphere that they attribute to ion-mediated nucleation.

1.1. Atmospheric Ions

[3] *Wilson*'s [1911] early work showed that ions are effective nucleating agents. Ions are likely aerosol pre-

[1]Also at Cooperative Institute for Research in the Environmental Sciences and Department of Chemistry and Biochemistry, University of Colorado, Boulder, Colorado, USA.

0148-0227/04/2003JD004460

cursors because they form very stable clusters, due to the strong electrostatic interaction with polar ligands. Ions are formed by cosmic rays at the rate of 1–30 ion pairs cm^{-3} s^{-1} in the background lower atmosphere with maximum rates at about 10 km [*Rosen et al.*, 1985]. Other ion sources, such as radioactive decay, lightning, transmission lines, and combustion, can produce locally elevated ion concentrations. The reactive ions (e.g., N_2^+, O_2^+, N^+, O^+) and electrons produced in the initial ionization of air are converted rapidly to cluster ions of protonated bases (e.g., $H_3O^+(H_2O)_n$, $(CH_3)_2COH^+(H_2O)_n$, and $NH_4^+(H_2O)_n$) and of the conjugate bases of strong acids (e.g., $NO_3^-(HNO_3)_x(H_2O)_y$) [*Ferguson*, 1979]. In the presence of the strong acid H_2SO_4, $NO_3^-(HNO_3)_x(H_2O)_y$ ions are converted to cluster ions of HSO_4^-. Ions are lost by recombination with ions of the opposite polarity, and by reaction with aerosol. Ion-ion recombination is the dominant ion loss process for aerosol surface areas below about 10 μm^2 cm^{-3}. For an ion production rate of 5 pair cm^{-3} s^{-1} and no background aerosol, the steady state ion concentration is about 1800 ions cm^{-3}, and the ion lifetime with respect to recombination is about 350 s. The ion production rate ultimately limits the maximum nucleation rate for IIN.

1.2. Gas Phase Nucleation: Neutrals and Ions

[4] At the molecular level, gas phase homogeneous nucleation involves a series of reversible elementary reactions leading from the gas phase molecules through molecular clusters to stable drops or crystals. The spontaneity of gas phase homogeneous nucleation is determined by the Gibbs free energy for formation of the relevant clusters from their gas phase constituents. Small clusters are generally less stable than the bulk because of limited solvation. Therefore, for moderate supersaturations, there is often a barrier on the Gibbs free energy surface for cluster growth. Gibbs free energy surfaces for the H_2SO_4/H_2O neutral and negative ion systems calculated with our kinetic model (vide infra) are shown for a specific set of conditions in Figure 1. For these conditions there is a significant barrier on the neutral coordinate, and no barrier on the negative ion coordinate. In this case, growth of the cluster ions is mostly limited by the rate of H_2SO_4 addition, whereas the initial growth of the neutral clusters is strongly inhibited due to efficient evaporation of the small clusters. The critical cluster, which sits on top of the barrier, has an effective vapor pressure equal to the partial pressure of the ligand (in this case, H_2SO_4). Clusters larger than the critical cluster grow spontaneously because the partial pressure of the ligand exceeds the effective vapor pressures of the clusters. The clusters that are smaller than the critical cluster have effective vapor pressures greater than the partial pressure of the ligand, and evaporation is spontaneous. Ion cluster growth will generally have smaller Gibbs free energy barriers than the corresponding neutral system due to the strong electrostatic interactions between the ion and the ligands. The height and position of the barrier are functions of the supersaturation. The barrier generally moves toward smaller clusters and decreases in height as the supersaturation increases. The rate of nucleation increases exponentially as the height of the barrier decreases.

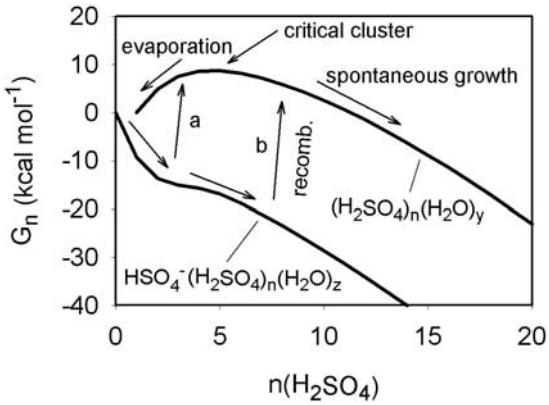

Figure 1. Gibbs free energy curves for the formation of neutral and ionic H_2SO_4/H_2O clusters for T = 253 K, RH = 0.55, and $[H_2SO_4] = 1.0 \times 10^7$ molecule cm^{-3}. Energies are averages over the H_2O coordinate, assuming that the clusters are equilibrated with H_2O. In pathway *a*, recombination of the cluster ion produces a neutral cluster smaller than the critical cluster, leading to cluster evaporation. Pathway *b* shows the IIN mechanism in which recombination produces a neutral cluster larger than the critical cluster, and growth is spontaneous.

[5] For atmospheric conditions (ion production rate = 1–30 ion pairs cm^{-3} s^{-1}, $[H_2SO_4] < 5 \times 10^7$ molecule cm^{-3}), cluster ions accumulate less than 100 sulfuric acid molecules before they are lost to recombination. Therefore the pathway for IIN involves ion cluster growth followed by recombination that produces a stable neutral cluster, larger than the critical cluster, that continues to grow [*Arnold*, 1980; *Turco et al.*, 1998]. This is an effective mechanism to bypass a nucleation barrier on the neutral coordinate (see pathway *b* in Figure 1).

[6] In classical nucleation theory, the thermodynamics of clusters are approximated with the liquid drop model [*Seinfeld and Pandis*, 1998] that assumes that the molecular clusters are spherical drops with surface tension and density equal to the bulk liquid. These assumptions are inappropriate for small molecular clusters, and lead to large uncertainties in nucleation rates derived from classical theory. For ionic clusters, the thermodynamics are calculated with the Thomson equation [*Holland and Castleman*, 1982], which approximates the ionic clusters as charged dielectric spheres with surface tension and density of the bulk liquid. Experimental studies have confirmed that the Thomson equation is generally not accurate for small ion clusters [*Holland and Castleman*, 1982].

[7] *Yu and Turco* [2001] and *Laakso et al.* [2002] have recently modeled the role of ions in the formation of particles in the troposphere. They conclude that the ionic mechanism is capable of explaining observations of tropospheric nucleation. However, their predictions have large uncertainties because the calculations are not based on accurate clustering thermodynamics.

2. Kinetic Model of Ion-Induced Nucleation

[8] An accurate kinetic treatment of atmospheric nucleation has not been possible due to a lack of thermody-

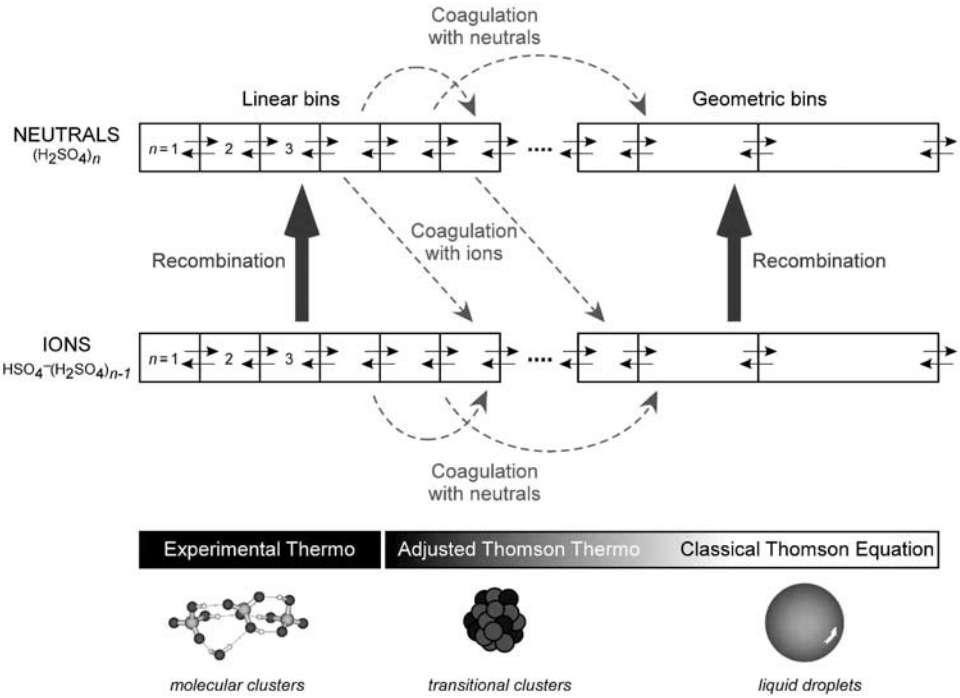

Figure 2. Schematic of the kinetic aerosol model depicting the time dependent evolution of ionic and neutral clusters in the H_2SO_4 coordinate. Arrows between adjacent bins represent H_2SO_4 condensation and evaporation. Clusters in each bin equilibrate with gas phase water. The kinetics for ion cluster growth and evaporation are derived from experimental thermodynamics for the small clusters ($HSO_4^-(H_2SO_4)_m(H_2O)_n$, m < 6) and the Thomson equation for large clusters (m > 30). The kinetics for the intermediate cluster ions are derived by interpolation.

namic data for the relevant clusters. We have implemented the following approach to significantly reduce uncertainties in the prediction of IIN rates in the H_2SO_4/H_2O system. (1) We have measured thermodynamics for the binding of H_2SO_4 and H_2O to cluster ions of the form $HSO_4^-(H_2SO_4)_x(H_2O)_y$ and $H^+(H_2SO_4)_n(H_2O)_m$. (2) We have connected the measured small cluster thermodynamics to the bulk liquid drop limit to yield thermodynamic predictions for all cluster sizes and compositions. (3) We have developed a nucleation model that treats the kinetics of growth and evaporation of neutral and ionic clusters explicitly.

2.1. Model Details

[9] Modeling H_2SO_4/H_2O binary nucleation is simplified by noting that the atmospheric water concentration is at least 10^4 times greater than the sulfuric acid concentration, so that the clusters equilibrate with water, and the growth and evaporation of the clusters is limited by addition and loss of H_2SO_4. Our thermodynamic measurements indicate that the positive ions are less likely to nucleate than the negative ions [*Froyd and Lovejoy*, 2003a], so the positive ions are treated as a single species, and the neutral and negative ion clusters are treated explicitly. The structure of the model is depicted schematically in Figure 2. For the neutral and negative clusters, the model uses 20–40 bins that increment by one sulfuric acid molecule, representing hydrated $(H_2SO_4)_n$ and $HSO_4^-(H_2SO_4)_{n-1}$, respectively. The molecular resolution of these bins gives a full kinetic treatment of nucleation. In the next 40–60 bins the number of sulfuric molecules increases geometrically, typically by a factor of 1.5 in order to account for particles up to about 1 μm diameter.

[10] All clusters equilibrate with water and grow and evaporate by addition and loss of H_2SO_4. Negative clusters coagulate with neutral clusters, recombine with positive ions, and are formed by the coagulation of smaller negative and neutral clusters. Neutral clusters coagulate with both neutral and negative clusters, and are formed by the recombination of cluster ions and by the coagulation of smaller neutral clusters. The differential equations describing condensation and evaporation of H_2SO_4 and coagulation are similar to the ones presented by *Raes and Janssens* [1986]. The temporal evolution of the neutral clusters starting with $(H_2SO_4)_2$ is given by

$$\begin{aligned}\frac{\partial[i]}{\partial t} = {} & \frac{k^d_{i+1}}{n_{i+1}-n_i}[i+1] - \frac{k^d_i}{n_i-n_{i-1}}[i] + \frac{k^a_{i-1}[H_2SO_4][i-1]}{n_i-n_{i-1}} \\ & - \frac{k^a_i[H_2SO_4][i]}{n_{i+1}-n_i} + \sum_l \sum_j k^c_{j,l}[j][l] \\ & \cdot \frac{\left((n_l+n_j)-n_{i-1}\right)}{(n_i-n_{i-1})}\delta_{n_l+n_j,[n_{i-1},n_i]} \\ & + \sum_l \sum_j k^c_{j,l}[j][l]\frac{\left(n_{i+1}-(n_l+n_j)\right)}{(n_{i+1}-n_i)}\delta_{n_l+n_j,[n_i,n_{i+1}]} \\ & - \sum_j k^c_{i,j}[i][j] - \sum_J k^c_{i,J}[i][J] + k^r_I[I][pos] \end{aligned} \quad (1)$$

The delta function is defined by

$$\delta_{n_l+n_j,[n_{i-1},n_i]} = \begin{array}{l} 0 \text{ if } n_l + n_j \notin [n_{i-1}, n_i] \\ 1 \text{ if } n_l + n_j \in [n_{i-1}, n_i] \end{array} \quad (2)$$

where n_i is the number of H_2SO_4 molecules in cluster i. Lowercase indices refer to neutral clusters, and uppercase indices refer to negative cluster ions. The first term on the right-hand side of equation (1) describes the production of neutral cluster i by the loss of an H_2SO_4 molecule from the next larger cluster (i + 1). The second term accounts for the loss of i due to evaporation of one H_2SO_4 molecule. The third term is the production of i by addition of H_2SO_4 to the next smaller cluster, and the fourth term is the loss of i by reaction with H_2SO_4. The fifth and sixth terms describe the production of i by coagulation of smaller neutral clusters. The seventh term is the loss of cluster i by coagulation with all other clusters, and the eighth term accounts for the loss of cluster i by coagulation with all of the negative clusters. The last term describes the gain of cluster i due to recombination of negative ion cluster I with a positive ion. It is assumed that the positive ions do not contain H_2SO_4, so that recombination of ion cluster I produces a neutral cluster i with the same number of H_2SO_4. Neutralization converts HSO_4^- to H_2SO_4.

[11] The evolution of the negative clusters starting with $HSO_4^- H_2SO_4$ is given by

$$\begin{aligned} \frac{\partial[I]}{\partial t} = {} & \frac{k^d_{I+1}}{n_{I+1} - n_I}[I+1] - \frac{k^d_I}{n_I - n_{I-1}}[I] + \frac{k^a_{I-1}[H_2SO_4][I-1]}{n_I - n_{I-1}} \\ & - \frac{k^a_I[H_2SO_4][I]}{n_{I+1} - n_I} + \sum_l \sum_J k^c_{J,l}[J][l] \\ & \cdot \frac{((n_l + n_J) - n_{I-1})}{(n_I - n_{I-1})} \delta_{n_l+n_J,[n_{I-1},n_I]} \\ & + \sum_l \sum_J k^c_{J,l}[J][l] \frac{(n_{I+1} - (n_l + n_J))}{(n_{I+1} - n_I)} \delta_{n_l+n_J,[n_I,n_{I+1}]} \\ & - \sum_j k^c_{I,j}[I][j] - k^r_I[I][pos] \end{aligned} \quad (3)$$

where the H_2SO_4 association and decomposition terms are similar to those of the neutrals. In contrast to the neutrals, the negative ions are produced by coagulation of negative with neutral clusters and lost by coagulation with only the neutrals. The negative clusters are also lost by recombination with positive ions.

[12] The temporal variation of the H_2SO_4 concentration is given by

$$\begin{aligned} \frac{\partial[H_2SO_4]}{\partial t} = {} & P_{H_2SO_4} + 2k^d_{(H_2SO_4)_2}\left[(H_2SO_4)_2\right] + \sum_j k^d_j[j] \\ & + \sum_J k^d_J[J] - 2k^a_i[H_2SO_4]^2 - \sum_j k^a_j[H_2SO_4][j] \\ & - \sum_J k^a_J[H_2SO_4][J] + k^r_{HSO_4^-}\left[HSO_4^-\right][pos] \\ & - k^a_{NO_3^-}\left[NO_3^-\right][H_2SO_4] \end{aligned} \quad (4)$$

The first term on the right-hand side is the photochemical production rate of H_2SO_4 (see below). The second term describes the production of H_2SO_4 from decomposition of the H_2SO_4 dimer. The third term describes the production from the evaporation of neutral clusters larger than the dimer, and the fourth term is the production from decomposition of the negative cluster ions. The fifth term accounts for the loss due to dimerization. The sixth and seventh terms describe the loss of H_2SO_4 due to condensation on neutral and negative clusters. The eighth term is the production of H_2SO_4 by neutralization of HSO_4^- and the last term is the loss of H_2SO_4 by reaction with the NO_3^- cluster ions.

[13] In the troposphere, the rate-limiting step for the production of gas phase H_2SO_4 is the reaction of OH with SO_2. The rate of production of H_2SO_4 ($k_{OH+SO2}[OH][SO_2]$) is closely coupled to the solar flux through the OH production. We use the OH + SO_2 rate coefficient recommended by *DeMore et al.* [1997]. The H_2SO_4 production rate is modeled with half a sinusoidal period extending from sunrise to sunset. The production rate of H_2SO_4 is given by

$$P_{H_2SO_4} = \delta_{t,[iD,iD+L]} M \sin\left(\frac{\pi(t - iD)}{L}\right) \quad (5)$$

The delta function ensures that the photochemical production of H_2SO_4 is zero at night, and is defined by

$$\delta_{t,[iD,iD+L]} = \begin{array}{l} 0 \text{ if } t \notin [iD, iD + L] \\ 1 \text{ if } t \in [iD, iD + L] \quad \text{for } i = 0, 1, 2, 3 \ldots \end{array} \quad (6)$$

where M is the maximum H_2SO_4 production rate, L is the time between sunrise and sunset, D is the length of the day (i.e., 24 hours), and i is the day index. Sunrise is at $t = iD$.

[14] As described in the introduction, atmospheric ionization produces unstable ions that rapidly convert to clusters based on the NO_3^- core ion. The model assumes that ion production starts with the NO_3^- cluster, which reacts with H_2SO_4 to produce the hydrated HSO_4^- ion. The variation of the NO_3^- cluster ions is given by

$$\begin{aligned} \frac{\partial\left[NO_3^-\right]}{\partial t} = {} & S_{ion} - k^r_{NO_3^-}\left[NO_3^-\right][pos] - k^a_{NO_3^-}[H_2SO_4]\left[NO_3^-\right] \\ & - \sum_j k^c_{NO_3^-,j}\left[NO_3^-\right][j] \end{aligned} \quad (7)$$

where S is the ion pair production rate, the second term is the NO_3^- cluster loss due to recombination, the third term accounts for loss via reaction with H_2SO_4, and the last term is the loss of NO_3^- by coagulation with the neutral clusters.

[15] The temporal variation of the HSO_4^- concentration is given by

$$\begin{aligned} \frac{\partial\left[HSO_4^-\right]}{\partial t} = {} & k^a_{NO_3^-}\left[NO_3^-\right][H_2SO_4] + k^d_{HSO_4^- H_2SO_4}\left[HSO_4^- H_2SO_4\right] \\ & - k^a_{HSO_4^-}[H_2SO_4]\left[HSO_4^-\right] - \sum_j k^c_{HSO_4^-,j}\left[HSO_4^-\right][j] \\ & - k^r_{HSO_4^-}\left[HSO_4^-\right][pos] \end{aligned} \quad (8)$$

[16] Here the first and second terms on the right-hand side are the production of HSO_4^- by reaction of NO_3^- clusters

with H_2SO_4 and by decomposition of $HSO_4^-H_2SO_4$. The third term is loss of HSO_4^- by association with H_2SO_4, the fifth term is loss by coagulation with all the neutral clusters starting with $(H_2SO_4)_2$, and the last term is loss due to recombination with positive ions.

[17] H_2SO_4 evaporation/decomposition rate constants (k^d) were calculated from the H_2SO_4 clustering thermodynamics and the condensation/association rate coefficient (k^a). For example, for the following reaction

$$HSO_4^-(H_2SO_4)_x(H_2O)_y + H_2SO_4 \rightleftharpoons HSO_4^-(H_2SO_4)_{x+1}(H_2O)_y \quad (9)$$

the H_2SO_4 condensation/association and evaporation/decomposition rate coefficients are related to the Gibbs free energy change by

$$\frac{k^a}{k^d} = K_c = RTe^{\frac{-\Delta G^\circ}{RT}} \quad (10)$$

where K_c is the equilibrium constant in concentration units and ΔG° is the Gibbs free energy change for the reaction. For each cluster, the equilibrium water distribution was calculated based on the ambient temperature, relative humidity, and measured water clustering thermodynamics. The effective H_2SO_4 condensation and evaporation rate coefficients were calculated by averaging the individual rate coefficients (e.g., for reaction (9)) over the equilibrium water distributions.

$$k_x^a = \sum_y f_{x,y} k_{x,y}^a \quad (11)$$

where $f_{x,y}$ is the fraction of the equilibrium distribution of a cluster with x H_2SO_4 that has y waters, and $k_{x,y}^a$ is the corresponding condensation rate coefficient. Similar averaging was performed to derive evaporation rate constants.

[18] Brownian coagulation coefficients (k^c) for neutral and charged particles were calculated by using Fuch's approach [*Fuchs*, 1964; *Seinfeld and Pandis*, 1998; *Yu and Turco*, 1998]. The ion-neutral coagulation coefficients were matched to the *Su and Chesnavich* [1982] prediction for the HSO_4^- + H_2SO_4 rate coefficient (k_{298K} = 2 × 10^{-9} cm^3 molecule^{-1} s^{-1}) by scaling the ion/dipole term in the interaction potential. Recombination coefficients were calculated with Fuch's Brownian coagulation formula for oppositely charged particles [*Fuchs*, 1964]. A value of 1.6 × 10^{-6} cm^3 molecule^{-1} s^{-1} was used for the small cluster limiting recombination coefficient [*Bates*, 1982]. Accomodation coefficients were typically set to 1.0 for H_2SO_4 condensation on neutral and negative clusters, and for coagulation of all clusters. Rate coefficients for association of H_2SO_4 to neutral and charged clusters, coagulation of neutral and charged clusters, ion-ion recombination, and decomposition are shown as a function of cluster size in Figure 3. Ion production rates as a function of altitude were taken from *Rosen et al.* [1985]. The set of differential equations describing cluster growth, evaporation, and coagulation was integrated by using a semi-implicit extrapolation method suitable for stiff sets of equations [*Press et al.*, 1992].

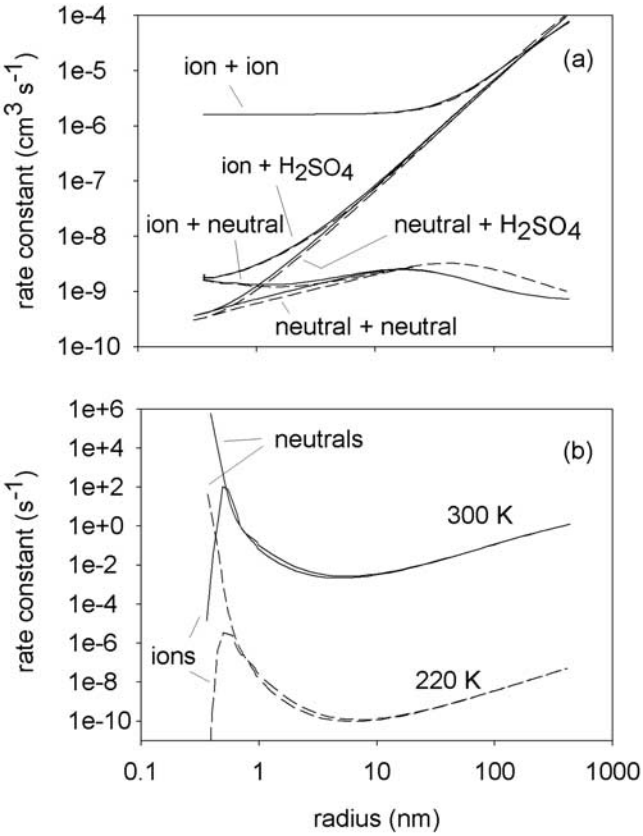

Figure 3. Model rate coefficients as a function of cluster size. Solid lines are for 300 K, 1013 mbar, and RH = 0.5, and dashed lines are for 220 K, 200 mbar, and RH = 0.5. (a) Ion-ion recombination, H_2SO_4 condensation, and coagulation rate coefficients for ionic and neutral clusters. The "ion + neutral" and "neutral + neutral" values are for clusters with an equal number of H_2SO_4 molecules. (b) Rate coefficients for evaporation of H_2SO_4 as a function of cluster size at 220 and 300 K.

2.2. Cluster Thermodynamics

[19] The growth and evaporation kinetics for the clusters were calculated from the cluster thermodynamics as described above. The enthalpy and entropy changes for the clustering reactions

$$HSO_4^-(H_2SO_4)_x(H_2O)_{y-1} + H_2O \rightleftharpoons HSO_4^-(H_2SO_4)_x(H_2O)_y \quad (12)$$

for $x \leq 6$ and $y \leq 10$ were derived from the temperature dependence of the equilibrium constants measured in an ion-molecule flow reactor coupled to a quadrupole mass spectrometer [*Froyd and Lovejoy*, 2003b]. The enthalpy changes for the sulfuric acid clustering reactions

$$HSO_4^-(H_2SO_4)_{x-1} + H_2SO_4 \rightleftharpoons HSO_4^-(H_2SO_4)_x \quad (13)$$

for $x \leq 5$ were derived from a master equation analysis of the temperature and pressure dependence of the thermal

decomposition reactions (13) measured in a quadrupole ion trap mass spectrometer [*Curtius et al.*, 2001; *Lovejoy and Curtius*, 2001]. Reaction entropies were calculated with standard formulae by using ab initio (HF/6 − 31 + G(d)) geometries and scaled vibrational frequencies [*Curtius et al.*, 2001]. The reaction enthalpies and entropies for sulfuric acid clustering to the hydrated clusters

$$HSO_4^-(H_2SO_4)_{x-1}(H_2O)_y + H_2SO_4 \rightleftharpoons HSO_4^-(H_2SO_4)_x(H_2O)_y \quad (14)$$

were derived from the experimental results for reactions (12) and (13) by using thermodynamic cycles. The experimental thermodynamics for the small cluster ions deviated significantly from the Thomson predictions, but converged towards the Thomson predictions for the larger clusters. The Thomson equation over predicted the water binding for the small clusters by up to 7 kcal mol^{-1}, and under predicted the sulfuric acid binding by up to 11 kcal mol^{-1}. The set of experimental cluster ion thermodynamics was connected to the Thomson predictions for larger clusters by adding small terms to the Thomson equation that decayed exponentially with cluster size. The details of the interpolation scheme are described by *Froyd* [2002]. This analysis yielded a complete set of H_2SO_4 and H_2O binding thermodynamics extending from molecular cluster ions to the bulk, based on experimental thermodynamics for the small clusters. Bulk liquid H_2SO_4/H_2O thermodynamics were derived from vapor pressures calculated with the On-line Aerosol Inorganics Model [*Carslaw et al.*, 1995]. The thermodynamics, density [*Perry and Chilton*, 1973], and surface tension [*Sabinina and Terpugow*, 1935] of bulk sulfuric acid-water solutions were parameterized as a function of composition and temperature.

[20] The thermodynamics of the neutral clusters are evaluated with the liquid drop model modified to give nucleation rates consistent with the experimental results of *Ball et al.* [1999]. The terms, $4\exp(-x/5)$ and $5\exp(-y/5)$ (units of kcal mol^{-1}), are added to the liquid drop Gibbs free energies for the addition of sulfuric acid and water, respectively, to the clusters $(H_2SO_4)_x(H_2O)_y$. These terms systematically decrease the bond energies of H_2SO_4 and H_2O and inhibit the neutral nucleation relative to predictions based on the liquid drop model. With these modifications, nucleation of the neutrals is negligible for the conditions examined in this study. The *Ball et al.* [1999] experiments were performed with H_2SO_4 concentrations significantly higher than found in the atmosphere. Therefore the predictions of the direct neutral nucleation with our model are quite uncertain due to the exponential dependence of the nucleation rate on the cluster thermodynamics. Conversely, the IIN rate is significantly less sensitive to the neutral thermodynamics. The IIN rate is sensitive to the position of the neutral nucleation barrier, which is a relatively weak function of the cluster thermodynamics (vide infra). The present modified liquid drop thermodynamics predict a neutral critical cluster containing 5 H_2SO_4 molecules for 1×10^7 H_2SO_4 cm^{-3}, RH = 0.5, and 240 K, which is consistent with measurements by *Eisele and Hanson* [2000], who report a critical cluster "near" 4 H_2SO_4 molecules.

3. Model Predictions for the Atmosphere

[21] Nucleation contour plots were generated by running the model from sunrise until sunset for a range of relative humidities, sulfuric acid source strengths, and preexisting aerosol surface areas. Results from about 1000 model runs were used to generate particle production contours for a given temperature. At a specific temperature, the particle production is most sensitive to RH and H_2SO_4 concentration. The H_2SO_4 concentration is a function of the H_2SO_4 production rate and the aerosol surface area, which is an important H_2SO_4 sink. To reduce the dimensionality of the system we plot the particle production contours as a function of RH and the average maximum daytime $[H_2SO_4]$. The averaging facilitates the representation of the data and introduces uncertainties in the particle production of typically less than 20%. We define the particle production as the sum of new particles greater than 3 nm diameter because this coincides with the minimum detectable size of the particle counters deployed in the field.

[22] Particle production contours for a range of temperatures characteristic of the troposphere are plotted in Figure 4. The concentration of H_2SO_4 is typically less than 10^8 molecule cm^{-3} in the boundary layer, and less than 10^7 in the middle and upper troposphere (see, e.g., Table 1). Based on these $[H_2SO_4]$, it is apparent that the $HSO_4^-/H_2SO_4/H_2O$ nucleation mechanism has the potential to produce more than 10^4 particles >3 nm per cubic centimeter in a day in the middle and upper troposphere.

[23] The rate of nucleation depends strongly on the thermodynamics for cluster growth. The position and height of the nucleation barrier is sensitive to the temperature, RH and $[H_2SO_4]$. Low temperatures, high RH, and high $[H_2SO_4]$ decrease the height of the barrier and facilitate nucleation. Figure 5 shows the conditions where the nucleation barrier for the ion coordinate is eliminated and the growth of all cluster ions is spontaneous. For example, for temperatures below 240 K and RH greater than 0.3 there is no barrier to ion growth for $[H_2SO_4]$ greater than about 10^6 molecule cm^{-3}.

[24] The minimum $[H_2SO_4]$ required to produce 100 particles in 12 hours of daylight is around 2×10^6 molecule cm^{-3} under the most favorable nucleation conditions (e.g., 220 K, see Figure 4). There is no barrier to IIN for these conditions (see Figure 5) and the particle production is determined by the rates of ion production and H_2SO_4 condensation. In the warm humid boundary layer, greater than 10^8 H_2SO_4 molecule cm^{-3} are required to make just 100 particles cm^{-3} in a day. There are barriers to nucleation for these conditions, and the particle production is a stronger function of temperature, RH, and $[H_2SO_4]$.

[25] The particle production by IIN is self-limiting. As the production rate increases, the surface area increases and eventually reaches levels where small particles are effectively scavenged and 3 nm particle production is suppressed. The maximum particle production rates are about 40,000 particle cm^{-3} day^{-1} with diameters greater than 3 nm for the conditions of Figure 4.

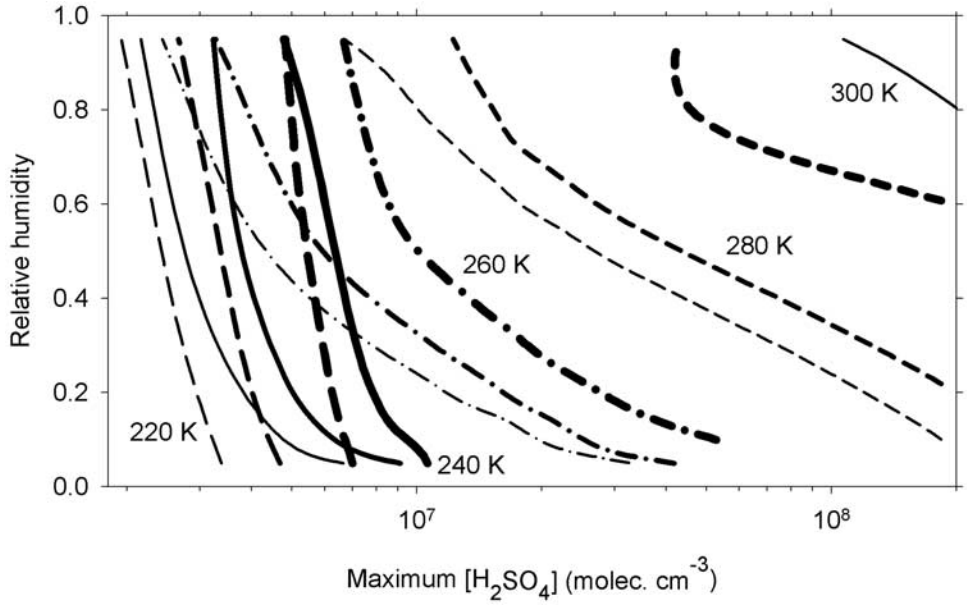

Figure 4. Particle production contours for a range of tropospheric temperatures. Thin/medium/thick lines represent conditions for the production of 100/1000/10000 particle cm^{-3} greater than 3 nm diameter in 12 hours. Long-dashed lines are 220 K, solid lines are 240 K, dashed-dot lines are 260 K, short-dashed lines are 280 K, and solid line is 300 K. Contours were derived from model calculations using initial aerosol surface areas ranging from 0 to 9 μm^2 cm^{-3} and midday H_2SO_4 production rates ranging from 100 to 18000 molecule cm^{-3} s^{-1}. Preexisting aerosol was modeled with a lognormal distribution peaked at 60 nm diameter and a geometric standard deviation of 1.8. RH is with respect to ice for T < 273 K. Ion pair production rates (34/32/17/6/2 cm^{-3} s^{-1} at 220/240/260/280/300 K) were derived from the measurements of *Rosen et al.* [1985] assuming a standard atmosphere.

[26] In this work, background particles are typically modeled with a lognormal distribution centered around 60 nm diameter. For typical atmospheric conditions, H_2SO_4 uptake to this aerosol is in the free molecular regime and the first order loss of H_2SO_4 is given approximately by the surface area times 5.5×10^{-5} s^{-1} um^{-2} cm^3.

3.1. Comparison With Observations

[27] *Weber et al.* [1999] recently summarized observations of middle and lower troposphere nucleation events that include measurements of ultrafine particles, H_2SO_4 concentration, RH and temperature. These data are tabulated in Table 1 with data for several other events published more recently. A direct comparison between the model predictions and observations is problematic because the history of the air parcel containing the fresh ultrafine particles is uncertain, and the range of observed conditions may not accurately represent the conditions during nucleation. We calculated particle production for the observations listed in Table 1 by running the model from sunrise until the observation time for RH's, surface areas, and H_2SO_4 production rates characteristic of the observation conditions (see Table 1). A contour plot of the particle production as a function of RH and [H_2SO_4] for the ACE 1 flight 27 nucleation event is presented in

Table 1. Observed and Predicted Particle Concentrations for Atmospheric Nucleation Events

Location	Ref.[a]	Altitude, km	[H_2SO_4], 10^6 cm^{-3}	RH, %	Temp., °C	Surface Area, μm^2 cm^{-3}	Local Time	Max. Observed Particle Concentration,[b] cm^{-3}	Model Predictions,[c] cm^{-3}
Mauna Loa Observatory	A	ground	7.8–9.5	49–53	11–12	4–18	1200	60 UF1	<1
Idaho Hill	B	ground	8.4–9.8	28–29	10	40–60	1200	200 UF1	<1
ACE 1	C	0.043	4.4	58	4.4		1316	400 UF1	<10
Macquarie Island		0.55	7.3	17	2.8		1325	2200 UF1	<10
PEM Tropics A Flight 19	D	0.16–0.18	3.7–55	88–98	23–25	7–15	1400	35 000 UCN	<1600
ACE 1 Flight 17	E	3.2–4.1	2.0–6.0	36–62	−11–−17	<10	1600–1800	4000 UF2, 10 000 UCN	<30 000
ACE 1 Flight 27	E	4.0–4.2	12–19	45–65	−19–−20	<12	1200–1400	2000 UF2, 6000 UCN	<35 000
ACE 1 Flight 16	F	5.8–6.0	1.5–2.5	30–80	−22–−24	2–8	1500–1600	230 UF1, 4000 UCN	<40 000
PEM Tropics B Flight 13	G	0.3	20–40	70–80	26	20–60	1230–1300	0 UF1, 400 UCN	<2000
		5.5	4–8	40–90	4–−8	5–20	1130–1230	6 UF1, 1200 UCN	<38 000

[a]A [*Weber et al.*, 1995]; B [*Weber et al.*, 1997]; C [*Weber et al.*, 1998]; D [*Clarke et al.*, 1998b]; E [*Clarke et al.*, 1998a]; F [*Weber et al.*, 2001a]; G [*Weber et al.*, 2001b].

[b]UF1 = 3–4 nm diameter; UF2 = 3–10 nm; UCN = >3 nm.

[c]UCN particle production predicted by the model. See text for details.

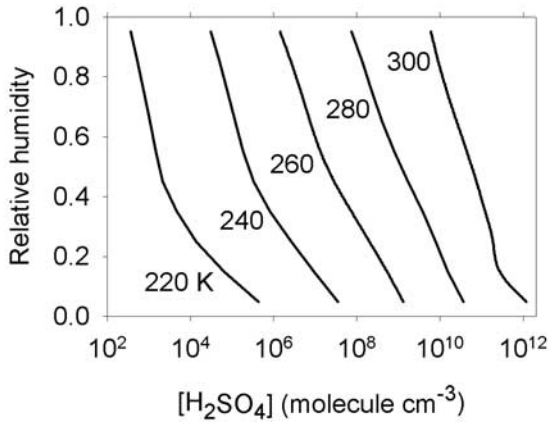

Figure 5. Conditions for elimination of the nucleation barrier for the $HSO_4^-/H_2SO_4/H_2O$ IIN pathway.

Figure 6. The model predicts up to 35 000 particle cm^{-3} greater than 3 nm diameter for these conditions, in agreement with the observed concentration of up to 6000 particle cm^{-3}. The temporal evolution of the H_2SO_4 and particle concentrations for a set of conditions characteristic of the flight 27 event is presented in Figure 7. For these conditions, the H_2SO_4 concentration peaks at 1.5×10^7 molecule cm^{-3} at about 1100 local time. The concentration of particles greater than 3 nm diameter reaches a maximum around 1400 hours at about 30 000 cm^{-3}. These particles appear over about 4 hours, giving apparent production rates of about 2 cm^{-3} s^{-1}. This is close to the limit dictated by the ion production rate of 5 ion pairs cm^{-3} s^{-1}. For these

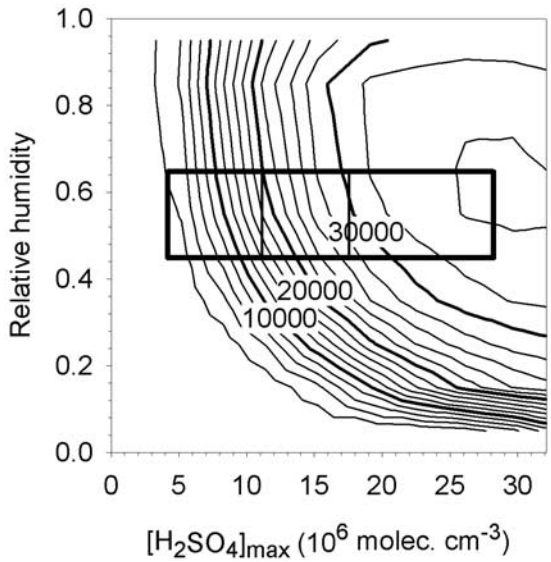

Figure 6. Predicted particle production for the ACE 1 flight 27 nucleation event as a function of the RH and maximum [H_2SO_4]. Model conditions: 253 K, 5 ion pair cm^{-3} s^{-1}, 100–4600 H_2SO_4 molecule cm^{-3} s^{-1} at noon, 15 hours of daylight, and 0–9 μm^2 cm^{-3} 60 nm diameter particles at sunrise. The inner box indicates the observed range of RH and [H_2SO_4]. The outer box shows the range of observed conditions including the uncertainty (2σ) in [H_2SO_4].

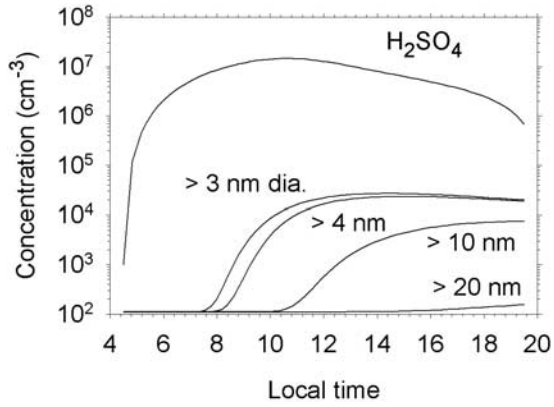

Figure 7. Temporal evolution of H_2SO_4 and ultrafine particles for conditions characteristic of the ACE1 flight 27 nucleation event (Table 1). Model conditions: 253 K, RH = 0.45, noontime H_2SO_4 production rate = 3000 molecule cm^{-3} s^{-1}, 15 hours of daylight, 5 ion pair cm^{-3} s^{-1}, surface area at sunrise = 2 μm^2 cm^{-3}, 60 nm diameter particles, surface area at sunset = 9 μm^2 cm^{-3}.

conditions there is no barrier to IIN for [H_2SO_4] above 6×10^6 molecule cm^{-3}.

[28] Similar analyses were performed for the other nucleation observations, and the predicted ranges of particle production are listed in Table 1. The wide range in the predictions is mostly a result of the sensitivity of the model to the [H_2SO_4] combined with relatively large uncertainties in [H_2SO_4]. Quoted uncertainties (2σ) in the H_2SO_4 measurements are ±42% for p > 940 mbar and ±62% for p < 940 mbar [*Mauldin et al.*, 1998].

[29] In general the model reproduces the observed particle production for events with atmospheric temperatures below about 270 K, but underpredicts the production for most of the lower-altitude, higher-temperature events. The low-altitude nucleation event observed during PEM Tropics B flight 13 is predicted by the model. This event had high [H_2SO_4] and surface areas, representative of very strong H_2SO_4 sources. The observed nucleation rates ($\sim$1 cm^{-3} s^{-1}) [*Weber et al.*, 1999] derived for the other low-altitude events and not predicted by the model, are comparable to ion production rates. These events may be due to an efficient ionic mechanism involving additional species (e.g., NH_3) or multicomponent neutral homogeneous nucleation [see, e.g., *Kulmala et al.*, 2000].

[30] Observations of new particle formation in the upper troposphere are not accompanied by measurements of H_2SO_4. *Hermann et al.* [2003] observed frequent enhanced concentrations of 4–9 nm particles in large regions of the upper troposphere, suggestive of widespread recent nucleation. *Schröder and Ström* [1997] observed bursts of >7 nm diameter aerosol in the midlatitude upper troposphere. In the absence of H_2SO_4 measurements, the propensity for IIN may be evaluated with Figure 8, which correlates particle production with the H_2SO_4 source strength and the preexisting aerosol surface area. For a typical midlatitude upper tropospheric noontime H_2SO_4 production rate of 700 molecule cm^{-3} s^{-1}, Figure 8 shows that IIN is important (>100 particle cm^{-3} day^{-1}) for surface areas below about 4 μm^2 cm^{-3}, consistent with the *Schröder*

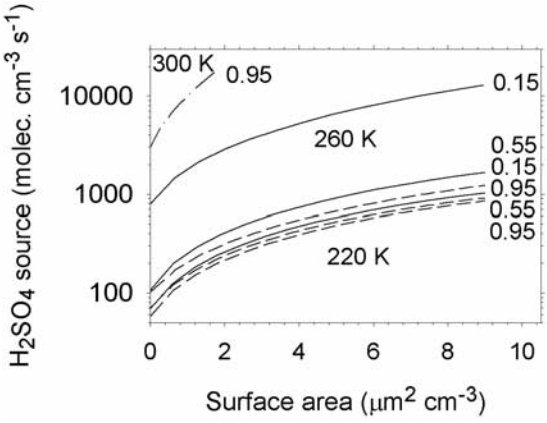

Figure 8. H_2SO_4 production rates and aerosol surface areas that lead to the formation of 100 new particles greater than 3 nm diameter in 12 hours for a range of temperature and relative humidity (0.15, 0.55, 0.95). Dashed lines are 220 K, solid lines are 260 K, and dashed-dot line is 300 K.

and Ström [1997] observations. The midday H_2SO_4 production rate was calculated for the following conditions: 220 K, 200 mbar, noontime [OH] = 0.4 pptv [*Brune et al.*, 1998] and [SO_2] = 30 pptv [*Thornton et al.*, 1999]. *Lee et al.* [2003] report good agreement between the predictions of our model and extensive observations of ultrafine particles in the upper troposphere and lower stratosphere, accompanied by measurements of OH and SO_2.

3.2. Comparison With Other Models

[31] *Yu and Turco* [2001] have simulated the *Clarke et al.* [1998b] PEM A observations of ultrafine particles in the marine boundary layer (see Table 1). Yu and Turco predict the formation of 2×10^4 particles cm^{-3} > 3 nm dia. in 4 hours for the following PEM A conditions: 298 K, RH = 0.95, 7 um^2 cm^{-3}, 10^4 H_2SO_4 cm^{-3} s^{-1}, and 2 ions cm^{-3} s^{-1}. Our model predicts <100 particle cm^{-3} in 12 hours for the same conditions. Similarly, comparisons with predictions by *Laakso et al.* [2002] for warm conditions show very different results. For example, for 293 K, RH = 0.5, 10 ion cm^{-3} s^{-1}, 2.3×10^4 H_2SO_4 cm^{-3} s^{-1} and clean air (about 1 um^2 cm^{-3}), *Laakso et al.* [2002] predict the production of >10^4 particles cm^{-3} in 3 hours. In contrast our model predicts <100 particle cm^{-3} in 12 hours. The large differences in the model predictions are not surprising considering the sensitivity of the rate of nucleation to the thermodynamics of the small cluster ions. *Yu and Turco* [2001] do not treat evaporation explicitly in their kinetic model, but scale the condensation rate coefficients to impose some resistance to cluster ion growth. *Laakso et al.* [2002] apply classical nucleation theory based on thermodynamics derived with the Thomson equation. The present work uses a full kinetic treatment of the condensation and evaporation of the cluster ions based on experimentally measured cluster ion thermodynamics.

3.3. Model Output Uncertainties

[32] Random, normally distributed errors of 0.5 kcal mol^{-1} in the Gibbs free energies of negative ion clustering lead to a standard deviation of 2% in the predicted number of particles greater than 3 nm diameter for the conditions of ACE 1 flight 27 (Table 1: T = 253 K, RH = 0.55, max. [H_2SO_4] = 1.1×10^7 molecule cm^{-3}). In this case, there is no barrier to nucleation and the nucleation rate is limited by the ion production and H_2SO_4 condensation, and is insensitive to the clustering thermodynamics. In contrast, when the particle production is less efficient, the model predictions are more sensitive to the clustering thermodynamics. For example, for conditions with net particle production of about 1000 particle cm^{-3} (253 K, RH = 0.55, max. [H_2SO_4] ≈ 5×10^6 molecule cm^{-3}), a 0.5 kcal mol^{-1} random uncertainty in the cluster ion thermodynamics leads to a 50% uncertainty in the particle production. The model predictions are relatively insensitive to the coagulation rate constants. Doubling the coagulation rate constants reduces the particle production (>3 nm diameter) by 15% for the conditions of the ACE 1 flight 27. Changing the sulfuric acid accommodation coefficient from 1.0 to 0.5 increases the [H_2SO_4] required for significant particle production (e.g., 1000 particles cm^{-3} > 3 nm dia.) by about two times, and decreases the net particle production at the highest productions (>10^4 cm^{-3}) by about a factor of two.

[33] The pathway for IIN involves ion cluster growth followed by recombination to produce a neutral cluster. If the resultant neutral cluster is smaller than the critical cluster it will evaporate, and if it is larger than the critical cluster it will continue to grow. Therefore the rate of IIN is a function of the size of the neutral critical cluster and is dependent on the neutral thermodynamics. Systematically making the neutral clusters all 1 kcal mol^{-1} less stable with respect to adding H_2SO_4 decreased the particle production by 20% for the conditions of ACE 1 flight 27 (T = 253K, RH = 0.55, max. [H_2SO_4] = 1.1×10^7 molecule cm^{-3}). At lower particle production rates (e.g., with T = 253 K, RH = 0.55, max. [H_2SO_4] = 5×10^6 molecule cm^{-3}) the particle production decreased by 50% for the same modification of the neutral thermodynamics as described above. These modifications of the neutral thermodynamics increased the size of the critical cluster ([H_2SO_4] = 5×10^6 molecule cm^{-3}) from 5 to 8 sulfuric acid molecules.

[34] It is recognized that sectional aerosol models are subject to errors associated with numerical diffusion [*Tsang and Rao*, 1988]. In this work, where the formation rate of 3 nm diameter particles is the main result, the errors are not significant because most of the particle growth and evaporation occur in the linear bins.

4. Summary

[35] We have developed a kinetic model of ion induced nucleation that is based on experimental thermodynamics of small ion clusters of H_2SO_4 and H_2O. This model should be a significant improvement over the current modeling strategies that are based on estimates of cluster thermodynamics. The model predicts that IIN of H_2SO_4 and H_2O is an efficient source of new particles in the middle and upper troposphere, thereby establishing links between particle formation and ions and H_2SO_4. Fossil fuel combustion is the major source of atmospheric SO_2, which directly impacts the H_2SO_4 production rate. In the free troposphere, ions are formed predominately by cosmic rays, which are modulated by solar activity [*Carslaw et al.*, 2002]. Therefore this work establishes a quantitative basis for under-

standing the influence of solar and anthropogenic activity on particle formation in the Earth's atmosphere.

[36] **Acknowledgments.** The authors are grateful to D. Hanson, R. Weber, and F. Eisele for useful discussions. This work was supported in part by NOAA's Climate and Global Change Program.

References

Arnold, F. (1980), Multi-ion complexes in the stratosphere—Implications for trace gases and aerosol, *Nature*, *284*, 610–611.

Ball, S. M., D. R. Hanson, and F. L. Eisele (1999), Laboratory studies of particle nucleation: Initial results for H_2SO_4, H_2O, and NH_3 vapors, *J. Geophys. Res.*, *104*, 23,709–23,718.

Bates, D. R. (1982), Recombination of small ions in the troposphere and lower stratosphere, *Planet. Space Sci.*, *30*, 1275–1282.

Brune, W. H., et al. (1998), Airborne in situ OH and HO_2 observations in the cloud-free troposphere and lower stratosphere during SUCCESS, *Geophys. Res. Lett.*, *25*, 1701–1704.

Carslaw, K. S., S. L. Clegg, and P. Brimblecombe (1995), A thermodynamic model of the system HCl-HNO_3-H_2SO_4-H_2O, including solubilities of HBr from <200 to 328 K, *J. Phys. Chem.*, *99*, 11,557–11,574. (Available at http://www.hpc1.uea.ac.uk/~e770/aim.html)

Carslaw, K. S., R. G. Harrison, and J. Kirby (2002), Cosmic rays, clouds, and climate, *Science*, *298*, 1732–1737.

Clarke, A. D. (1992), Atmospheric nuclei in the remote free-troposphere, *J. Atmos. Chem.*, *14*, 479–488.

Clarke, A. D. (1993), Atmospheric nuclei in the Pacific midtroposphere: Their nature, concentration, and evolution, *J. Geophys. Res.*, *98*, 20,633–20,647.

Clarke, A. D., J. L. Varner, F. Eisele, R. L. Mauldin, D. Tanner, and M. Litchy (1998a), Particle production in the remote marine atmosphere: Cloud outflow and subsidence during ACE 1, *J. Geophys. Res.*, *103*, 16,397–16,409.

Clarke, A. D., et al. (1998b), Particle nucleation in the tropical boundary layer and its coupling to marine sulfur sources, *Science*, *282*, 89–92.

Coffman, D. J., and D. A. Hegg (1995), A preliminary study of the effect of ammonia on particle nucleation in the marine boundary layer, *J. Geophys. Res.*, *100*, 7147–7160.

Covert, D. S., V. N. Kapustin, P. K. Quinn, and T. S. Bates (1992), New particle formation in the marine boundary layer, *J. Geophys. Res.*, *97*, 20,581–20,589.

Curtius, J., K. D. Froyd, and E. R. Lovejoy (2001), Cluster ion thermal decomposition (I): Experimental kinetics study and ab initio calculations for HSO_4^- $(H_2SO_4)_x$ $(HNO_3)_y$, *J. Phys. Chem. A*, *105*, 10,867–10,873.

DeMore, W. B., S. P. Sander, D. M. Golden, R. F. Hampson, M. J. Kurylo, C. J. Howard, A. R. Ravishankara, C. E. Kolb, and M. J. Molina (1997), Chemical kinetics and photochemical data for use in stratospheric modeling, *JPL Publ.*, *97-4*.

de Reus, M., J. Ström, M. Kulmala, L. Pirjola, J. Lelieveld, C. Schiller, and M. Zöger (1998), Airborne aerosol measurements in the tropopause region and the dependence of new particle formation on preexisting particle number concentration, *J. Geophys. Res.*, *103*, 31,255–31,263.

Eichkorn, S., S. Wilhelm, H. Aufmhoff, K. H. Wohlfrom, and F. Arnold (2002), Cosmic ray-induced aerosol formation: First observational evidence from aircraft-based ion mass spectrometer measurements in the upper troposphere, *Geophys. Res. Lett.*, *29*(14), 1698, doi:10.1029/2002GL015044.

Eisele, F. L., and D. R. Hanson (2000), First measurement of prenucleation molecular clusters, *J. Phys. Chem. A*, *104*, 830–836.

Ferguson, E. E. (1979), *Kinetics of Ion-Molecule Reactions*, edited by P. Ausloos, pp. 377–403, Plenum, New York.

Froyd, K. D. (2002), Ion induced nucleation in the atmosphere: Studies of NH_3, H_2SO_4, and H_2O cluster ions, Ph.D. thesis, Univ. of Colo., Boulder.

Froyd, K. D., and E. R. Lovejoy (2003a), Experimental thermodynamics of cluster ions composed of H_2SO_4 and H_2O. 1. Positive ions, *J. Phys. Chem. A*, *107*, 9800–9811.

Froyd, K. D., and E. R. Lovejoy (2003b), Experimental thermodynamics of cluster ions composed of H_2SO_4 and H_2O. 2. Measurements and ab initio structures of negative ions, *J. Phys. Chem. A*, *107*, 9812–9824.

Fuchs, N. (1964), *The Mechanics of Aerosols*, Macmillan, Old Tappan, N. J.

Harrison, R. G., and K. S. Carslaw (2003), Ion-aerosol-cloud processes in the lower atmosphere, *Rev.Geophys.*,*41*,1012, doi:10.1029/2002RG000114.

Hegg, D. A., L. F. Radke, and P. V. Hobbs (1990), Particle production associated with marine clouds, *J. Geophys. Res.*, *95*, 13,917–13,926.

Hegg, D. A., R. J. Ferek, and P. V. Hobbs (1993), Aerosol size distributions in the cloudy atmospheric boundary layer of the North Atlantic Ocean, *J. Geophys. Res.*, *98*, 8841–8846.

Hermann, M., J. Heintzenberg, A. Wiedensohler, A. Zahn, G. Heinrich, and C. A. M. Brenninkmeijer (2003), Meridional distributions of aerosol particle number concentrations in the upper troposphere and lower stratosphere obtained by Civil Aircraft for Regular Investigation of the Atmosphere Based on an Instrument Container (CARIBIC) flights, *J. Geophys. Res.*, *108*, 4114, doi:10.1029/2001JD001077.

Holland, P. M., and A. W. Castleman Jr. (1982), The Thomson equation revisited in light of ion-clustering experiments, *J. Phys. Chem.*, *86*, 4181–4188.

Hoppel, W. A., G. M. Frick, J. W. Fitzgerald, and R. E. Larson (1994), Marine boundary layer measurements of new particle formation and the effects nonprecipitating clouds have on aerosol size distribution, *J. Geophys. Res.*, *99*, 14,443–14,460.

Hõrrak, U., J. Salm, and H. Tammet (1998), Bursts of intermediate ions in atmospheric air, *J. Geophys. Res.*, *103*, 13,909–13,915.

Keil, A., and M. Wendisch (2001), Bursts of Aitken mode and ultrafine particle observed at the top of continental boundary layer clouds, *J. Aerosol Sci.*, *32*, 649–660.

Kulmala, M., L. Pirjola, and J. M. Mäkelä (2000), Stable sulfate clusters as a source of new atmospheric particles, *Nature*, *404*, 66.

Kulmala, M., H. Vehkmamäki, T. Petäjä, M. Dal Maso, A. Lauri, V.-M. Kerminen, W. Birmili, and P. H. McMurry (2004), Formation and growth rates of ultrafine atmospheric particles: A review of observations, *J. Aerosol Sci.*, *35*, 143–176.

Laakso, L., J. M. Mäkelä, L. Pirjola, and M. Kulmala (2002), Model studies of ion-induced nucleation in the atmosphere, *J. Geophys. Res.*, *107*, 4427, 10.1029/2002JD002140.

Lee, S. H., J. M. Reeves, J. C. Wilson, D. E. Hunton, A. A. Viggiano, T. M. Miller, J. O. Ballenthin, and L. R. Lait (2003), Particle formation by ion nucleation in the upper troposphere and lower stratosphere, *Science*, *301*, 1886–1889.

Lovejoy, E. R., and J. Curtius (2001), Cluster ion thermal decomposition (II): Master equation modeling in the low-pressure limit and fall-off regions—Bond energies for HSO_4^- $(H_2SO_4)_x$ $(HNO_3)_y$, *J. Phys. Chem. A*, *105*, 10,874–10,883.

Marti, J. J., A. Jefferson, X. P. Cai, C. Richert, P. H. McMurry, and F. Eisele (1997), H_2SO_4 vapor pressure of sulfuric acid and ammonium sulfate solutions, *J. Geophys. Res.*, *102*, 3725–3735.

Mauldin, R. L., III, G. J. Frost, G. Chen, D. J. Tanner, A. S. H. Prevot, D. D. Davis, and F. L. Eisele (1998), OH measurements during the First Aerosol Characterization Experiment (ACE 1): Observations and model comparisons, *J. Geophys. Res.*, *103*, 16,713–16,729.

Perry, K. D., and P. V. Hobbs (1994), Further evidence for particle nucleation in clear air adjacent to marine cumulus clouds, *J. Geophys. Res.*, *99*, 22,803–22,818.

Perry, R. H., and C. H. Chilton (1973), *Chemical Engineers' Handbook*, 5th ed., McGraw-Hill, New York.

Press, W. H., S. A. Teukolsky, W. T. Wetterling, and B. T. Flannery (1992), *Numerical Recipes in Fortran 77: The Art of Scientific Computing*, Cambridge Univ. Press, New York.

Raes, F., and A. Janssens (1986), Ion-induced aerosol formation in a H_2O-H_2SO_4 system-II. Numerical calculations and conclusions, *J. Aerosol Sci.*, *17*, 715–722.

Rosen, J. M., D. J. Hofmann, and W. Gringel (1985), Measurements of ion mobility to 30 km, *J. Geophys. Res.*, *90*, 5876–5884.

Sabinina, A. L., and L. Terpugow (1935), Die oberflächenspannung de systems schwefelsäure-wasser, *Z. Phys. Chem. A*, *173*, 237–241.

Schröder, F., and J. Ström (1997), Aircraft measurements of submicrometer aerosol particles (>7 nm) in the midlatitude free troposphere and tropopause region, *Atmos. Res.*, *44*, 333.

Seinfeld, J. H., and S. N. Pandis (1998), *Atmospheric Chemistry and Physics*, John Wiley, Hoboken, N. J.

Su, T., and W. J. Chesnavich (1982), Parametrization of the ion-polar molecule collision rate constant by trajectory calculations, *J. Chem. Phys.*, *76*, 5183.

Thornton, D. C., A. R. Bandy, B. W. Blomquist, A. R. Driedger, and T. P. Wade (1999), Sulfur dioxide distribution over the Pacific Ocean 1991–1996, *J. Geophys. Res.*, *104*, 5845–5854.

Tsang, T. H., and A. Rao (1988), Comparison of different numerical schemes for condensational growth of aerosols, *Aerosol Sci. Technol.*, *9*, 271–277.

Turco, R. P., J.-X. Zhao, and F. Yu (1998), A new source of tropospheric aerosol: Ion-ion recombination, *Geophys. Res. Lett.*, *25*, 635–638.

Weber, R. J., P. H. McMurry, F. L. Eisele, and D. J. Tanner (1995), Measurement of expected nucleation precursor species and 3-500-nm diameter particles at Mauna Loa Observatory, Hawaii, *J. Atmos. Sci.*, *52*, 2242–2257.

Weber, R. J., J. J. Marti, P. H. McMurry, F. L. Eisele, D. J. Tanner, and A. Jefferson (1997), Measurements of new particle formation and

ultrafine particle growth rates at a clean continental site, *J. Geophys. Res.*, *102*, 4375–4385.

Weber, R. J., P. H. McMurry, L. Mauldin, D. J. Tanner, F. L. Eisele, F. J. Brechtel, S. M. Kreidenweis, G. L. Kok, R. D. Schillawski, and D. Baumgardner (1998), A study of new particle formation and growth involving biogenic and trace gas species measured during ACE 1, *J. Geophys. Res.*, *103*, 16,385–16,396.

Weber, R. J., P. H. McMurry, R. L. Mauldin III, D. J. Tanner, F. L. Eisele, A. D. Clarke, and V. N. Kapustin (1999), New particle formation in the remote troposphere: A comparison of observations at various sites, *Geophys. Res. Lett.*, *26*, 307–310.

Weber, R. J., G. Chen, D. D. Davis, R. L. Mauldin III, D. J. Tanner, F. L. Eisele, A. D. Clarke, D. C. Thornton, and A. R. Bandy (2001a), Measurements of enhanced H_2SO_4 and 3–4 nm particles near a frontal cloud during the First Aerosol Characterization Experiment (ACE 1), *J. Geophys. Res.*, *106*, 24,107–24,117.

Weber, R. J., K. Moore, V. Kapustin, A. Clarke, R. L. Mauldin, E. Kosciuch, C. Cantrell, F. Eisele, B. Anderson, and L. Thornhill (2001b), Nucleation in the equatorial Pacific during PEM-Tropics B: Enhanced boundary layer H_2SO_4 with no particle production, *J. Geophys. Res.*, *106*, 32,767–32,776.

Wilson, C. T. R. (1911), On a method of making visible the paths of ionising particles, *Proc. R. Soc. London, Ser. A*, *85*, 285–288.

Yu, F., and R. P. Turco (1998), The formation and evolution of aerosols in stratospheric aircraft plumes: Numerical simulations and comparisons with observations, *J. Geophys. Res.*, *103*, 25,915–25,934.

Yu, F., and R. P. Turco (2001), From molecular clusters to nanoparticles: Role of ambient ionization in tropospheric aerosol formation, *J. Geophys. Res.*, *106*, 4797–4814.

J. Curtius, Institut für Physik der Atmosphäre, Universität Mainz, D-55099 Mainz, Germany.

K. D. Froyd and E. R. Lovejoy, Aeronomy Laboratory, NOAA, Boulder, CO 80305, USA. (nlovejoy@al.noaa.gov)